WIND FARM LAYOUT OPTIMIZATION WITH WAKES FROM FLUID DYNAMICS SIMULATIONS

Jonas Schmidt
Fraunhofer IWES, Oldenburg, Germany
jonas.schmidt@iwes.fraunhofer.de

Bernhard Stoevesandt
Fraunhofer IWES, Oldenburg, Germany
bernhard.stoevesandt@iwes.fraunhofer.de

Abstract:

Twelve actuator disk CFD simulations of an isolated rotor were carried out, whose setups differ only by a variation of the inflow wind profile and derived quantities. By interpolating the resulting set of velocity deficit fields to arbitrary inflow wind speeds at hub height, a CFD based numerical wake model was obtained. This model was compared to wake models from the literature, using the new wind farm modelling software `flapFOAM`. It was found that the outcome of a gradient-based wind farm layout optimization depends on the choice of wake model. For the CFD wake model, different wake overlap models were compared to full farm CFD simulations. While the total deficit of a row of turbines is described well, the total deficit between column organized turbines is underestimated by `flapFOAM`.

Keywords: Wind farms, wake models, layout optimization, computational fluid dynamics

1 Introduction

Wake models play a major role during the optimization of wind farm layouts. They mediate the interaction between the turbines, and are therefore decisive for calculations of the park efficiency, turbine loads and other observables with wind farm modelling codes. In this work we describe a method which is suitable for obtaining new wake models from pre-calculated computational fluid dynamics (CFD) simulations, and discuss their inclusion into the newly developed software `flapFOAM`.

Wind farm modelling software has been developed since more than two decades, for scientific and commercial applications. Examples are `PARK/UPMWAKE` [1] and `WAsP` [2] (DTU, Danmark), `FarmFlow` [3] (ECN, Netherlands), `WindFarmer` [4] (GH, United Kingdom) and the Farm Layout Proframm `FLaP` [5] (University of Oldenburg, Germany). `flapFOAM` follows some of the concepts of `FLaP`, without sharing code, and couples them to the open source CFD tool box `OpenFOAM` [6].

Two of the oldest wake models are the Jensen model [7] and the Ainslie model [8], and they are still widely used. A number of new and improved models have been developed since, based on different simplifying assumptions, cf. the reviews [9, 10]. Often the models include parameters that are determined empirically. Notice that if enough data is available, it is also possible to build wake models that are fully based on data analysis [11].

For a fixed layout and fixed inflow conditions, the wake effect within a wind farm can be studied in detail by CFD methods. This is computationally demanding, and also here modelling issues occur, like the choice of turbulence model and wall functions, or the rotor representation.

A linearized CFD model for wake calculations, which is using look-up tables and has with very short computation time, was developed under the name `Fuga` at DTU [12]. This model is integrated into `WAsP`, and also gave rise to a new parametrized wake model [13].

Here we follow a different path towards the integration of CFD simulations into wind farm modelling. Based on a data base of single rotor CFD results, we develop a new numerical wake model that is on the same footing as analytical wake mod-

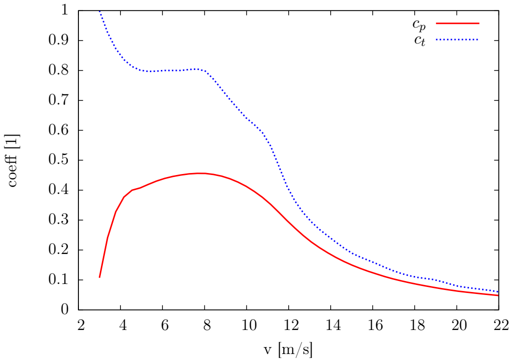

Figure 1: *The power and thrust coefficient curves for the model turbine.*

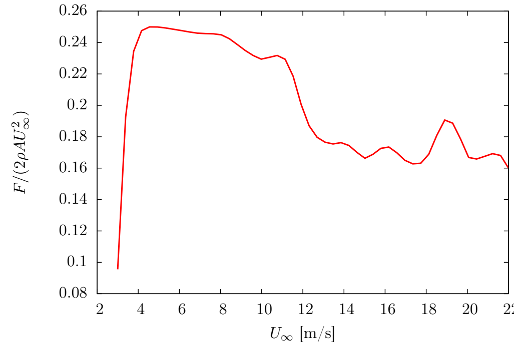

Figure 2: *The normalized axial disk force for the model turbine.*

els. Although it may be time consuming to provide that data base, this work has only to be done once for a given setting. The wake calculation inside the wind farm is then reduced to reading and interpolating the pre-calculated CFD velocity fields.

The paper is organized as follows. In Section 2 the new CFD wake model is described, for concreteness based on a set of specific actuator disk simulations. Section 3 then gives an overview of the methods implemented in `flapFOAM`, and results obtained with this software for different wake models are shown in Section 4. The findings are discussed in Section 5, before we conclude in Section 6.

2 Numerical wake model based on CFD simulations

Numerical simulations of the wake of an isolated turbine can only be carried out for discrete sets of inflow conditions. Non-CFD wind farm modelling, on the other hand, relies on wake models that yield velocity deficits for continuous inflow wind speeds, since in wind farm situations the local conditions include effects of wakes from upstream turbines. In the following a wake model that matches this requirement is developed, based on the numerical interpolation of discrete sets of wake deficit fields. The latter are obtained from steady single wake CFD simulations.

2.1 Single rotor CFD simulations

An isolated model wind turbine with 3.2 MW rated power, 123 m hub height and $D = 114$ m rotor diameter is represented by a uniform actuator disk model. The disk force is strictly in the axial direction and has the integrated magnitude

$$F = 2\rho A a(1-a)U_\infty^2, \qquad (1)$$

with undisturbed axial wind speed U_∞, air density ρ, rotor area A and $a = 1 - c_p/c_t$, where c_p and c_t are the power and thrust coefficients, respectively. For their dependence on U_∞, the power and thrust curves from Fig. 1 were assumed, implying the axial force shown in Fig. 2. The actuator disk from `OpenFOAM` (version 2.1.1) was modified such that the undisturbed wind speed U_∞ is adopted during the simulation from the velocity at a point of fixed upstream distance on the rotor axis.

For the single wake simulations steady incompressible Reynolds-Averaged-Navier-Stokes (RANS) equations were solved with `OpenFOAM` (version 2.1.1). Turbulence closure was obtained by invoking the $k-\epsilon$ model with increased dissipation near the rotor, as proposed by El Kasmi and Masson [14].

The computational domain has dimensions 5500 m $\times$ 1000 m $\times$ 500 m. The mesh is hexadominant with 8.2×10^5 cells, it is shown in Fig. 4 together with two nested refinement boxes and the resulting actuator disk cells. The latter consists of 4872 cells. Grid independency was checked by comparing the centre line velocity for four different meshes and $U_\infty = 10$ ms^{-1} at hub height, shown in Fig. 3.

The boundary conditions at the inflow patch at the west describe a neutral ABL log-profile with roughness length $z_0 = 0.05$ m. The turbulent kinetic energy k was fixed by the requirement of 10% ambient turbulence intensity at the inflow. The turbulent dissipation ϵ was taken from the Richards-Hoxey solu-

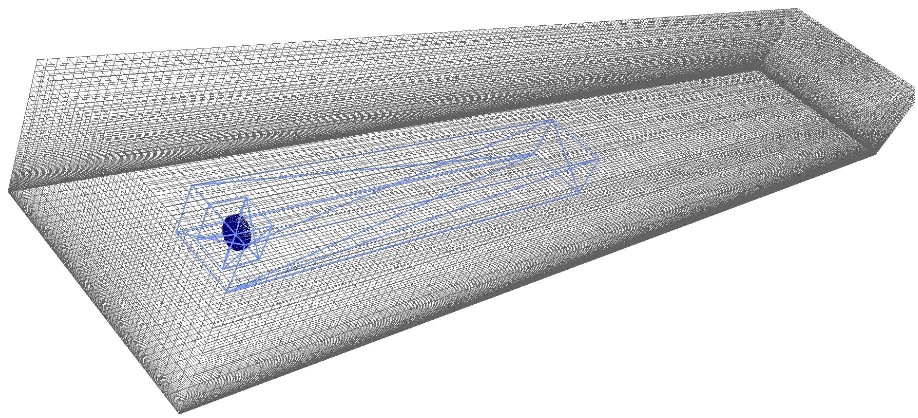

Figure 4: *The mesh used for single rotor simulations, refinement boxes and the cells of the actuator disk.*

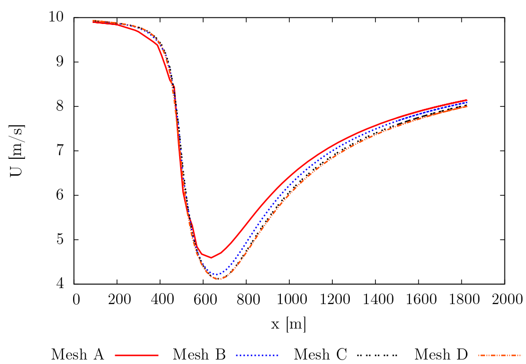

Figure 3: *The centre line axial velocity for* $U_\infty = 10$ *ms*$^{-1}$ *at hub height and four different meshes. Meshes A, B, C and D have* 3×10^4, 2.5×10^5, 8.2×10^5 *and* 1.9×10^6 *cells, respectively. All subsequent simulations are done with mesh C, shown in Fig. 4.*

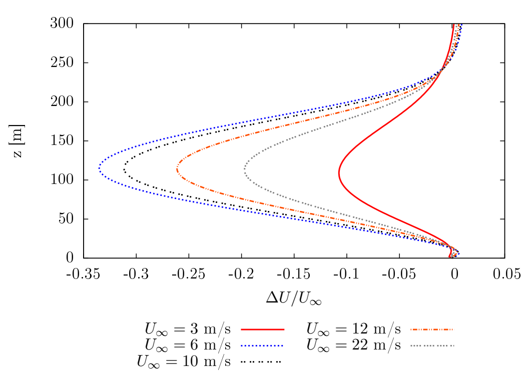

Figure 5: *Simulated axial velocity deficits along a vertical line through a point on the rotor axis at downstream distance* $5D$ *from the rotor, for a subset of the inflow wind speeds (2).*

tion [15], with constant parameter $C_\mu = 0.033$. At the ground patch wall functions were used, and slip conditions at side and top patches.

Twelve steady RANS simulations were carried out for inflow wind speeds

$$U_\infty = 3, 4, 5, 6, 8, 10, 11, 12, 13, 15, 18, 22 \text{ m s}^{-1} \quad (2)$$

at hub height. This distribution represents a set of support points of the axial disk force curve shown in Fig. 2, which has a significant drop at the onset of the pitch region near $U_\infty = 11$ m s^{-1}. All fields of all simulations carried out for this work converged with residuals below 10^{-5}.

We define the velocity deficit field as

$$\Delta U = U - U_0, \quad (3)$$

where U_0 is the velocity field from the pure ABL background simulation, ie., the same simulation as described above with the rotor switched off. The axial deficits along a vertical line through the rotor axis at downstream distance $5D$, where D is the rotor diameter, is shown in Fig. 5 for a subset of the inflow wind speeds (2).

2.2 Velocity deficit interpolation

The setup of the simulations described in the previous section differs by only one parameter, the inflow wind speed at hub height U_∞. The resulting set of velocity deficit fields can hence be understood as discrete data on a non-equidistant one-dimensional grid. For such type of data, numerical interpolation and differentiation to any order of accuracy can be achieved by following Fornberg [16], whose algorithm we implemented in C++. This allows us to

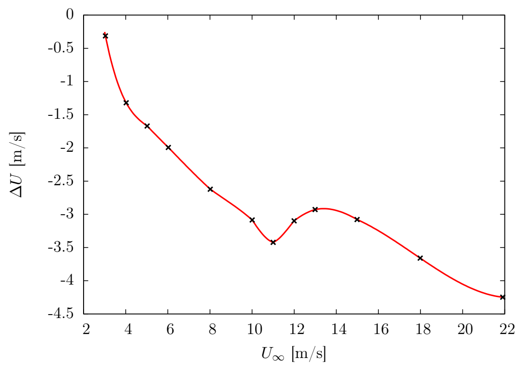

Figure 6: *Velocity deficit in x direction at a point on the rotor axis with downstream distance $5D$ from the rotor. The crosses mark simulation results.*

interpolate the velocity deficit ΔU from the discrete simulated data (2) to continuous inflow wind speeds in the range

$$3 \text{ m s}^{-1} \leq U_\infty \leq 22 \text{ m s}^{-1}. \tag{4}$$

An example is shown in Fig. 6, where the velocity deficit was interpolated at a point $5D$ downstream on the rotor axis. Notice the local minimum around $U_\infty = 11$ m s^{-1}, which reflects the onset of the pitch region, cf. Fig. 2.

This field-valued interpolation is sufficient for the definition of a wake model based on any pre-calculated set of steady single rotor simulations. Notice that all input data that enters the CFD simulations, apart from U_∞, plays the role of fixed wake model parameters, including the rotor model.

3 The wind farm modelling software `flapFOAM`

The new software `flapFOAM`, developed at Fraunhofer IWES, is intended to be used for wind farm modelling and layout optimization. It follows a similar approach as the wind farm layout program FLaP [5], but is fully embedded into the framework of `OpenFOAM`. This extends the modelling possibilities, since the code is fully written in C++ and can easily be extended by new models due to its modular structure. Notice that currently only flat terrain is supported. A first validation of the code with laboratory data was carried out in [17], see also the discussion in Section 5. A detailed description of the full scope, the implementation and the usage of `flapFOAM` will be given elsewhere.

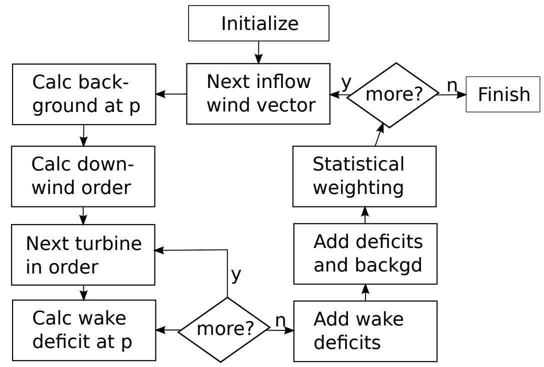

Figure 7: *Principle flow chart of the calculation of the wind velocity at a point p with `flapFOAM`.*

3.1 Calculation of the wake effect

The basic principle of `flapFOAM` is the local superposition of a background wind field and velocity deficits due to the wakes in the wind farm. The logic of the calculation of the wind velocity vector at an arbitrary point p inside the wind farm is shown in Fig. 7.

For any calculation, a so called 'inflow case' has to be specified. It defines the distribution of the backgrounds of interest, over which the results will be averaged. This includes the option to study single-state cases as well as the definition of a wind rose with specific distributions of wind speed and wind direction within each sector. The background wind fields can be uniform, horizontal wind profiles, or fields from steady CFD simulations. Wind distributions and the wind rose can also be read from met mast or simulated data.

Different strategies for the determination of the downwind order of the wind turbines are implemented, ranging from pure background field analysis to iterative methods. The local overlap of velocity deficits at a point is then calculated by so called 'wake addition models'. Currently the options are the naive deficit vector addition (dubbed 'add' in the following), or the subsequent rescaling to the square root of the sum of deficit squares ('sqrtSqr'), or the averaging of the deficits ('av'). The contributions from upstream turbines are then added subsequently, subject to the rules of the selected wake addition model.

A clear distinction is made between wind fields and wind fields that are conditioned on one continuous parameter. The latter are dubbed 'wind field entities'. An example is the velocity deficit field describing the wake of an isolated wind turbine; its local value at a point behind the rotor depends on the inflow wind speed at an upstream reference point. A wake model in `flapFOAM` is therefore defined as a wind field entity whose reference parameter is the effective axial inflow wind velocity U_∞.

The calculation of the latter for each turbine of the wind farm is coupled to the calculation of the downwind order, and the results are stored until either the background wind conditions or the turbine positions change. The set of points at which the wind field is evaluated for this calculation is determined by so-called 'rotor models'. In the simplest case, only the wind velocity at the geometrical centre of the rotor is considered, more complicated models involve disk averages. Notice that back reaction effects between the wake and the background wind field, as in CFD simulations, do not occur, thus the reference points can be chosen to lie in the rotor plane.

The resulting effective axial inflow wind speed is also used for the calculation of the power produced by the wind turbine. This is implemented in a 'machine model', and currently only the direct evaluation of the power curve is available.

3.2 Wake models

In `flapFOAM` each wind turbine is equipped with a wake model. It is therefore possible to select different models or different model parameters, depending on the position in the wind farm. Currently, five different wake models are implemented. For a summary of the corresponding model equations, see the appendix of Ref. [17].

Jensen model

The Jensen model wake is characterised by linear wake expansion as a function of the downstream distance from the rotor plane [7], with a proportionality constant $k = 0.04 \ldots 0.07$. Only the axial velocity deficit is modelled, with the magnitude obtained by momentum conservation. The deficit is constant in the radial direction within the wake, and abruptly drops to zero at its boundary.

Frandsen model

The wake model by Frandsen et al. [18] was developed for describing the wake inside a wind farm. Three regimes of the wake are modelled, the single-wake regime, which is the only one that is currently implemented in `flapFOAM`, the multiple-wake regime and the boundary-layer regime. Similar to the Jensen model only the horizontal component of the velocity is modelled. The profile is hat-shaped at constant downwind distance from the rotor, ie., it is independent of the radial coordinate inside the wake. The growth of the wake radius is not linear in the single-wake regime but a function of the thrust coefficient of the rotor.

Larsen model

The Larsen model [19] assumes an axisymmetric wake, reducing the RANS equations to two dimensions. For the Reynolds stresses Prandtl's mixing length theory is applied [20]. Empirical model constants are determined by comparison to measurements at $9.5D$ behind an isolated turbine. The wake radius is given as an explicit non-linear function of the downwind coordinate in this model. Horizontal and radial velocity components are described, they possess dependencies on the downstream and radial coordinates. The wake expansion and decay are determined by the thrust coefficient and the ambient turbulence intensity. The Larsen model has analytical solutions at first and second order with respect to an expansion in the axial velocity deficit.

Ainslie model

Like the Larsen model, the Ainslie model [8] is based on the assumption of an axisymmetric wake. Turbulence closure is obtained by an eddy-viscosity model. Up to $2D$ downwind distance from the rotor the wake is set to a Gaussian profile, before it starts evolving according to the two coupled partial differential equations in the radial and downwind coordinates. Parameters are the thrust coefficient and ambient turbulence, the latter entering the eddy viscosity components. The solutions for the axial and radial velocity components are obtained numerically on a two dimensional grid, by mapping the discretized equations to a tri-diagonal matrix problem. In `flapFOAM` this is solved on demand, the results are stored in a data base. Also the options for the Ainslie filter function, a contribution from ambient turbulence intensity to the eddy viscosity, and Vermeulen's near wake length are implemented, following [5], but they are not considered in the results shown here.

CFD based wake model

Any discrete set of steady single rotor simulations can be used to generate a wake model in `flapFOAM`, as described in Section 2.2. In the following the actuator disk model from Section 2 will be used as an example, and for comparison a model equipped with the standard $k-\epsilon$ turbulence model that is otherwise identical.

3.3 Layout optimization

The optimization of the layout of a wind farm at a given site is the search for an extremum of an objective function, which may be composed of the total energy production of the wind farm, the expected loads, inter-turbine cable length and other cost factors. Some of these and additional requirements can also be formulated as constraints, like spatial restrictions or maximal sound levels at given points of interest. The parameter space is high dimensional and scaling with the number of turbines. In principle, also tower heights and machine characteristics like thrust curve control points may be chosen as variables for research and development purposes.

Currently, the optimization strategy in `flapFOAM` is based on the constraint function minimization algorithm `CONMIN` [21], which was implemented in C++. This gradient-based algorithm can be combined with random initial conditions search. A coupling of `flapFOAM` and the open source optimization tool box `DAKOTA` [22] is work in progress.

For this work, we restrict the optimization to wind farm energy maximization and geometrical constraints. The main purpose here is to study wake models and their effect on wind farm calculations and layout optimization, not the influence of objective functions, constraints, and the optimization strategy on wind farm layouts.

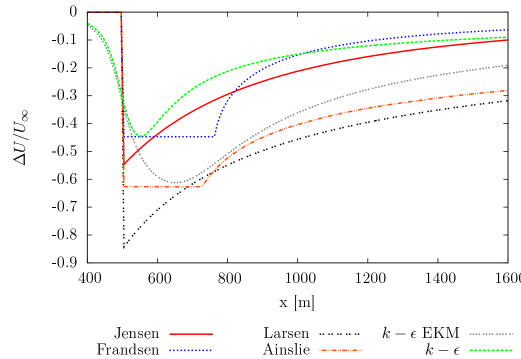

Figure 8: *Axial velocity deficit at hub height. The turbine is located at $x = 500$ m, the inflow wind speed at hub height is $U_\infty = 8$ m s^{-1}.*

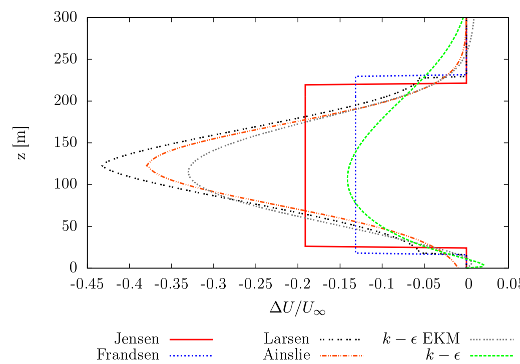

Figure 9: *Axial velocity deficit at downwind distance $5D$ from the rotor centre. The inflow wind speed at hub height is $U_\infty = 8$ m s^{-1}.*

4 Results

4.1 Single rotor wakes

The velocity deficits in x-direction along the symmetry axis of a single rotor with centre at $x = 500$ m and hub height 123 m, according to the different wake models described in Sec. 3.2, are shown in Fig. 8. Notice the spread of the deficits, and the qualitative differences in the near wake region.

The corresponding deficit profiles along a vertical line crossing the rotor axis at distance $5D$ downstream of the rotor centre for the same settings are shown in Fig. 9. Notice the 'hat-shaped' profiles of the Jensen and Frandsen models.

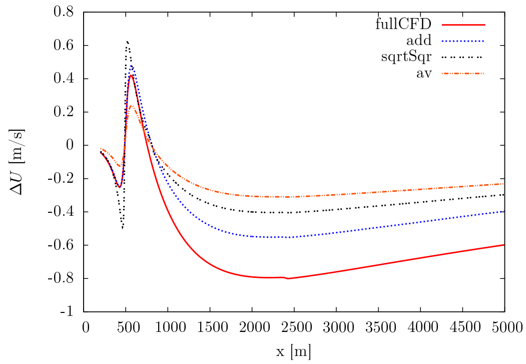

Figure 10: *The velocity deficit in x-direction along the symmetry line between two identical model turbines at hub height, for inflow $U_\infty = 10$ m s^{-1}. The lines compare 'wake addition models' of `flapFOAM` with a full CFD simulation. The chosen wake model and the actuator disk model are described in Sec. 2.1.*

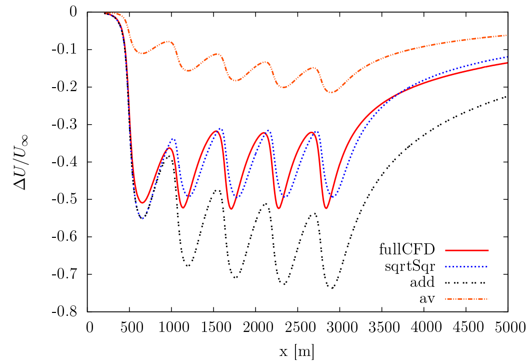

Figure 11: *The velocity deficit in x-direction along the symmetry axis of five rotors in a row with spacing $5D$, for the `flapFOAM` 'wake addition models' and the full farm CFD simulation. The chosen wake model and the actuator disk model are described in Sec. 2.1.*

4.2 Wake overlap

The performance of the wake addition models is evaluated by comparing the results of the `flapFOAM` CFD wake model from Sec. 2.1 to full CFD RANS actuator disk simulations.

The first test case consists of two identical model turbines of hub height 123 m, located at positions $x = 500$ m, $y = 1000$ m $\pm D$. For model turbines and the wind profile described in Sec. 2, with wind velocity vectors parallel to the x-axis and magnitude 10 m s^{-1} at hub height, the results of the comparison are shown in Fig. 10. For the CFD, the computational volume was doubled compared to the single rotor mesh, with 1.3 mio. cells in total. All three 'wake addition models', which either add the deficits (line 'add'), consider the average deficit (line 'av') or the square root of the sum of deficit squares (line 'sqrtSqr') underestimate the combined deficit. The simple addition of deficits gives the best results, with error of 2% relative to the inflow wind speed.

The second test case consists of 5 identical wind turbines at positions $x = 500$ m $+ 5nD$, where $n = 0, \ldots, 4$ labels the rotors. The results for the different 'wake addition models' are shown in Fig. 11. Here the addition of square roots of deficit squares is found to perform best, compared to the full farm CFD simulation. We also implemented a switch that ignores upstream turbines beyond the dominant rotor during the deficit summation, but this did not improve the results and is not included here.

4.3 Layout optimization

The findings of wind farm layout optimization depend on the applied wake model. For a test farm of four turbines, initially in a row, and the different `flapFOAM` wake models, the optimal layouts according to the gradient-based optimizer are compared in Fig. 12. Here the optimization parameters and the uniform inflow with wind speed $U_\infty = 8$ m s^{-1} were kept constant. In addition to the geometrical farm boundary constraints, a minimal inter-turbine distance of 500 m was imposed. The 'wake addition model' was 'sqrtSqr', the local inflow velocity was averaged over a disk with four radial and four azimuthal sectors for each turbine.

For the Jensen wake model and the CFD wake model from Sec. 2.2, the velocity deficits in x-direction at hub height are shown in Figs. 13 and 14, respectively. Notice that the Jensen model, and also the Frandsen model, have no radial dependency within the wake regime, therefore the gradient optimizer fails to find the global minimum. Similarly, in the CFD wake model case, two neighbouring wakes are preventing turbine number 3 from finding a position with undisturbed inflow. However, the centre wake regions are escaped successfully, due to the radial decreasing velocity deficit in these models. This is likewise observed for the Ainslie and Larsen wake models.

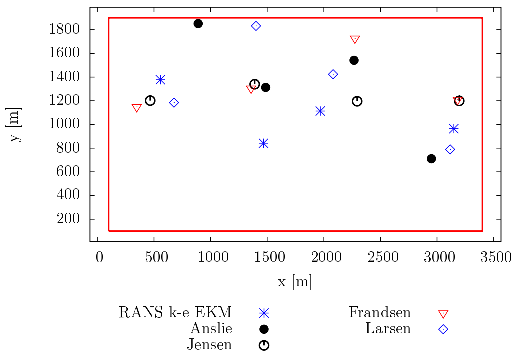

Figure 12: *Optimization results for an initial row of four turbines in the x-direction, which is the uniform flow direction. The inflow wind speed was $U_\infty = 8$ m s^{-1}. The 'wake addition model' was 'sqrtSqr', the downwind order method iterative.*

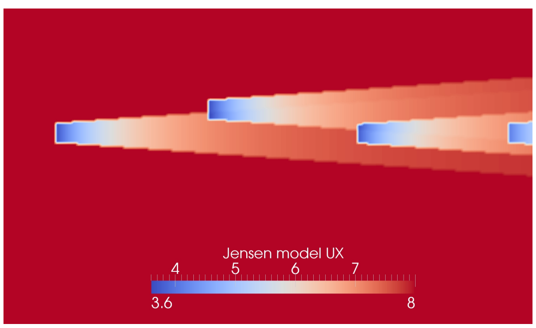

Figure 13: *Optimization results for an initial row of four turbines in the x-direction, which is the uniform flow direction, and the Jensen wake model.*

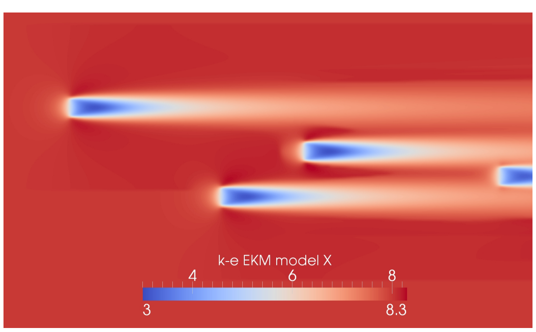

Figure 14: *Optimization results for an initial row of four turbines in the x-direction, which is the uniform flow direction, and the CFD wake model from Sec. 2.2.*

5 Discussion

The wind farm modelling approach that is followed here is based on the overlap of single rotor wake deficits. Figures 8 and 9 demonstrate that wake models have a broad spread in the predicted velocity deficits, due to parameter choices and model assumptions.

With the method described in Sec. 2.2 we were able to contribute a new class of wake models, based on pre-calculated steady CFD simulations of a single rotor. Notice the significant effect of the additional dissipation in the near rotor reagion of the El Kasmi and Masson turbulence model, compared to the standard $k-\epsilon$ model, as it was expected according to [14]. For a first validation of `flapFOAM` with a laboratory scale model turbine, see reference [17]. A validation with measurement data from MW-scale turbines is so far lacking and therefore left for future work.

Our approach differs from the `FUGA` model from DTU, which is an unconventional linearized and therefore fast CFD model which also makes use of pre-calculated look-up tables [12], and is integrated into the wind farm modelling software `WAsP` [2]. Here full non-linear three-dimensional CFD results are combined to define a wake model, and the preparation of such a model needs some computational effort. However, once the model is set up, the model evaluation is fast and, possibly after a mapping to an appropriate grid, independent of the complexity of the underlying CFD. Notice that sufficient random access memory (RAM) is required to load the set of velocity fields that define the model.

Apart from the single wake model, the overlap prescription that determines how several wake deficits and a background field are to be superposed is the second crucial ingredient for the modelling of the wind field in a wind farm. In `flapFOAM` this is called a 'wake addition model', and three different models are compared in Figures 10 and 11. While the latter shows an acceptable agreement of the full farm CFD actuator disk simulation and the CFD based wake model for the model 'sqrtSqr', Figure 10 does not confirm this result. The overlap of wakes of turbines from two neighbour rows in an array, which are not affected by the each other's wakes, is not captured well by the implemented models. Here an error of 2.5% of the velocity deficit relative to the inflow wind speed can be expected for the model 'sqrtSqr', compared to the full farm CFD simulation. A further investigation and an improvement of the 'wake addition models' is neccessary.

For wind farm layout optimization, currently a gradient-based optimization method is implemented in `flapFOAM`. For wake models with constant deficits in the radial direction, like the Jensen or the Frandsen model, this has the drawback that turbines can get stuck within a wake, cf. Fig. 13. For more complicated wake models with radial deficit variation, like the Ainslie, the Larsen or the CFD wake models, this problem is evaded. However, turbines can be trapped in local minima between two wakes, cf. Fig. 14. This demonstrates that for wind farm layout optimization it is necessary to either combine the gradient method with random initial positioning, or to implement a genetic algorithm or alternative global optimization strategies. For `flapFOAM`, a coupling to the open source optimization tool box `DAKOTA` [22] is planned to overcome this issue.

FIgure 12 demonstrates that for identical optimizer and wake overlap settings, different wake models lead to different optimization results. This stresses the importance of wake model validation, for realistic turbines. Similarly, the choice of 'wake addition models' has an influence on the layout, and also here further research and validation projects are crucial. For realistic applications, the objective and constraint functions need to reflect the needs and interests of wind farm planers, and `flapFOAM` with its modular structure provides interfaces for such generalizations.

6 Conclusion

A lot of physics enters the calculation of the power output of a wind farm. It is the aim of the newly developed code `flapFOAM` to provide an extendable modelling platform that is able to represent as much of this as possible, and to perform wind farm calculations and layout optimization for various distributions of inflow conditions. `flapFOAM` is based on `OpenFOAM` libraries and fully programmed in C++. All implemented models are run-time selectable, and the code is easily extendable by new models.

Similar to what is done in other wind farm modelling software, the local wind velocity at a point inside the wind farm is obtained by overlapping a background wind field and the wake deficits that arise from upstream turbines. Each turbine is equipped with a wake model, and various models from the literature have been implemented.

The main point of this paper is to demonstrate that it is possible to obtain new numerical wake models from pre-calculated steady single rotor CFD simulations, and to use them in a wind farm modelling and optimization code. For this a set of actuator disk simulations was generated, for settings that only vary in the inflow velocity profile and derived quantities. By considering the value of the inflow wind speed at hub height as a single parameter, the set of simulations could be interpreted as data on an arbitrarily spaced grid in one dimension, and therefore interpolated to continuous values. In the future one may consider extending this approach to more dimensions, for example by including turbulence intensity as an independent local inflow parameter.

The above procedure closes the gap between engineering wake models and CFD simulations. All knowledge and experience from CFD rotor modelling can be transferred to wind warm layout optimization and other wind farm issues that rely on fast calculations. The new CFD engineering wake models are based on reading and interpolating existing results, therefore the run time is in principle independent of the degree of complexity of the underlying CFD. Thus also time averaged LES simulations could be used to define a wake model in `flapFOAM`, without increasing computation time compared to the corresponding RANS simulations.

This work is a proof-of-concept, and the development of `flapFOAM` is ongoing. It was shown that the wake overlap models underestimate the combined velocity deficit of two turbines in free-stream conditions. Furthermore, global optimization algorithms are required, since the gradient-based approach often leads undesired trapping of turbines between wakes. Finally, after a first validation with a laboratory-scale model turbine, detailed comparison of calculated results with wind farm data is urgently needed and work in progress.

Acknowledgements

The work is conducted in the scope of the project GW Wakes funded by the Federal Ministry for the Environment, Nature Conservation and Nuclear Safety (FKZ 0325397A). We would like to thank Carlos Peralta and Cherif Mihoubi for helpfull `OpenFOAM` model modifications and the optimization code, respectively. We also thank the computer time provided by the Facility for Large-scale Computations in Wind Energy Research (FLOW) at the

University of Oldenburg, Germany.

References

[1] A. Crespo et al. Numerical analysis of wind turbine wakes. In *Delphi Workshop on Wind Energy Applications, Delphi, Greece*, 1985.

[2] N.G. Mortensen and Risø National Laboratory. *Getting Started with WAsP 9*. Risø-I-2571. Risø National Laboratory, 2007.

[3] R.J. Barthelmie et al. Analytical modelling of large wind farm clusters. In *EAWE*, 2004.

[4] P.J. Eecen. Wind farm calculation and optimization with farmflow. In *Dutch Wind Workshop*, 2010.

[5] B. Lange, H. P. Waldl, A. G. Guerrero, D. Heinemann, and R. J. Barthelmie. Modelling of offshore wind turbine wakes with the wind farm program flap. *Wind Energy*, 6(1):87–104, 2003.

[6] OpenFOAM. http://www.openfoam.org, 2013. [Online; accessed 05-November-2013].

[7] J. O. Jensen. A note on wind generator interaction. Technical Report Risø-M-2411, Risø National Laboratory, 1983.

[8] J. F. Ainslie. Development of an eddy viscosity model for wind turbine wakes. In *BWEA Wind Energy Conference*, Oxford, UK, 1983.

[9] L. J. Vermeer, N. J. Srensen, and A. Crespo. Wind turbine wake aerodynamics. *Progress in Aerospace Sciences*, 39:467–510, 2003.

[10] S. T. Frandsen. The making of a second-generation wind farm eciency model-complex. *Wind Energy*, 12:445–458, 2009.

[11] N.G. Nygaard. Construction and validation of a new offshore wake model. In *ICOWES conference, Lyngby, DK*, 2013.

[12] Søren Ott, Morten Nielsen, Jacob Berg, and Hans Ejsing Jørgensen. *FUGA - A linearised CFD model tool for offshore wind farm wakes*. European Wind Energy Association (EWEA), 2011.

[13] O. S. Rathmann, S. Ott, and M. Kelly. Wind farm wake effects estimations by a mosaic tile wake model. In *EWEA*, 2011.

[14] A. El Kasmi and C. Masson. An extended model for turbulent flow through horizontal-axis wind turbines. *Journal of Wind Engineering and Industrial Aerodynamics*, 96(1):103–122, 2008.

[15] P. J Richards and R. P. Hoxey. Appropriate boundary conditions for computational wind engineering models using the $k-\epsilon$ turbulence model. *Journal of Wind Engineering and Industrial Aerodynamics*, 46-47(0):145–153, 1993. Proceedings of the 1st International on Computational Wind Engineering.

[16] Bengt Fornberg. Generation of finite difference formulas on arbitrarily spaced grids. *Mathematics of Computation*, 51(184):699–706, 1988.

[17] Stanislav Rockel, Elisabeth Camp, Jonas Schmidt, Joachim Peinke, Raulan Cal, and Michael Holling. Experimental study on influence of pitch motion on the wake of a floating wind turbine model. *Submitted for publication in Energies*, 2014.

[18] S. Frandsen, R. Barthelmie, S. Pryor, O. Rathmann, S. Larsen, J. Højstrup, and M. Thøgersen. Analytical modelling of wind speed deficit in large offshore wind farms. *Wind Energy*, 9:39–53, 2006.

[19] G. C. Larsen. A simple wake calculation procedure. Technical Report Riso-M-2760, Risø National Laboratory, 1988.

[20] L. M. Swain. On the turbulent wake behind a body of revolution. *Proc. Roy. Soc. Lond. A*, 125:647–659, 1929.

[21] G. N. Vanderplaats. Conmin - a fortran program for constrained function minimization user's manual. Technical Report NASA TM X-62,282, NASA Technical Memorandum, 1973.

[22] Adams et. al. Dakota, a multilevel parallel object-oriented framework for design optimization, parameter estimation, uncertainty quantification, and sensitivity analysis: Version 5.4 user's manual. Technical Report SAND2010-2183, Sandia Technical Report, 2009.